



# EFFECT OF LOADING RATE ON MECHANICAL BEHAVIOR OF CFRP LAMINATES

Shinji Ogihara\*, Hidenari Ogata\*\*, Koichiro Toda\*\* and Asao Koike\*\*\*

\* Department of Mechanical Engineering, Tokyo University of Science,

\*\* Graduate Student, Tokyo University of Science,

\*\*\* Isuzu Advanced Engineering Center, Ltd.

**Keywords:** *mechanical property, unidirectional laminates, cross-ply laminates, loading rate effect, one-parameter plasticity model, laminate theory*

## Abstract

*It is known that the mechanical behavior of CFRP laminates depends on the loading rate because of the properties of the matrix polymer. Therefore, it is very important to understand the effect of loading rate on the mechanical properties of CFRP laminates. The effect of strain rate on mechanical response of CFRP laminates is evaluated experimentally. A material system used was T700S/2500 carbon epoxy system. The loading-unloading tests as well as the monotonic tensile test are performed to divide the total strain into elastic and inelastic ones. Moreover, high strain-rate tests were carried out using a Split Hopkinson Pressure Bar (SHPB) technique. An attempt was made to model stress-inelastic strain relation by a viscoplasticity model based on one-parameter plasticity model for unidirectional laminates. Here, an attempt is made to predict stress-strain relation for the cross-ply laminate by combining viscoplastic models for the unidirectional laminate with the laminate theory.*

## 1 Introduction

It is known that the mechanical behavior of CFRP laminates depends on the loading rate because of the properties of the matrix polymer. Therefore, it is very important to understand the effect of loading rate on the mechanical properties of CFRP laminates to improve the design accuracy of the CFRP structure. Many mechanical models have been proposed to model the effect of loading rate on composite mechanical behavior, using two approaches, one macroscopic and the other

microscopic. In the macroscopic approach, composites are treated as a nonlinear elastic or plastic body. In the microscopic approach, attempts are made to describe the effective composite response using the properties of the fiber and matrix. This study describes the mechanical behavior of a unidirectional and a cross-ply CFRP laminates under on- and off-axis tensile loading at various loading rates. A material system used was T700S/2500 carbon epoxy system. Laminate configurations are unidirectional and cross-ply (0/90)<sub>s</sub>. Loading angles are 0°, 15°, 30°, 45°, 60°, 75° and 90° for unidirectional laminates, and 0°, 15°, 30°, 45° and 90° for cross-ply laminates. To measure both strains in the longitudinal and transverse directions, biaxial strain gages are put on the center part of the specimens. The loading-unloading test as well as monotonic tensile test was performed to divide the total strain into elastic and inelastic ones. Moreover, high strain-rate tests were carried out using a Split Hopkinson Pressure Bar (SHPB) technique. An attempt was made to model stress-inelastic strain relation by a viscoplasticity model based on one-parameter plasticity model for unidirectional laminates.

## 2 Experimental Method

### 2.1 Specimen

A material system used was T700S/2500 carbon epoxy system. Laminate configurations were unidirectional and cross-ply (0/90)<sub>s</sub>. Loading angles were 0°, 15°, 30°, 45°, 60°, 75° and 90° for unidirectional laminates, and 0°, 15°, 30°, 45° and 90° for cross-ply laminates.

## 2.2 Monotonic tensile test

Unidirectional specimen for monotonic tensile test was 300mm long and 10mm wide. The crosshead speed was 0.5mm/min., 5.0mm/min. and 50.0mm/min for unidirectional laminates. To measure both strains in the longitudinal and transverse directions, biaxial strain gages were put on the center part of the specimens for monotonic tensile test.

## 2.3 Loading-unloading test

Cross-ply specimen for loading-unloading test was 300mm long and 10mm wide. The crosshead speed was 0.5mm/min. and 5.0mm/min. for cross-ply laminates. To measure both strains in the longitudinal and transverse directions, biaxial strain gages were put on the center part of the specimens for loading-unloading test. The loading-unloading test as well as the monotonic tensile test were performed to divide the total strain into elastic and inelastic ones.

## 2.4 SHPB impact tensile test

Fig.1 shows schematic diagram of SHPB apparatus. A cylindrical striker impacts the flange and causes an elastic tensile loading wave to propagate along the input bar towards the specimen and output bar. The specimen is fixed with adhesive into parallel-side slots in the loading bars. Strain gage signals from two stations on the input bar and one on the output bar allow the full dynamic stress-strain curve to be derived using the standard Hopkinson-bar analysis [1]. Unidirectional SHPB impact tensile test specimens were 70mm long and 5mm wide. Uniaxial strain gages were put on the center part of the specimen for SHPB impact tensile test. To measure stress-strain relation of strain rate about 100/s, the SHPB impact tensile test was performed.

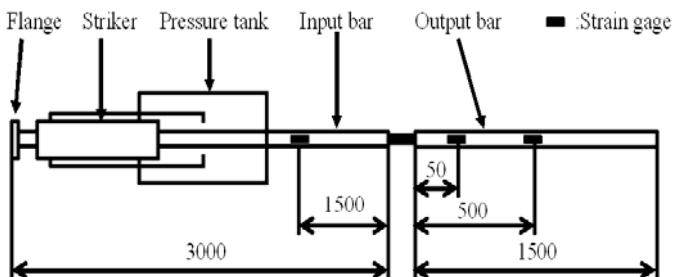


Fig.1 Schematic diagram of Split Hopkinson Pressure Bar apparatus.

## 3 Result and Discussion

### 3.1 Stress-strain curves

The measurement theory of the SHPB method is shown.

A cylindrical striker impacts the flange and causes an elastic tensile loading wave to propagate along the input bar. This wave propagates toward the incident bar –specimen interface, recorded by the strain gage, and is denoted by  $\varepsilon_i(t)$  and termed as incident wave. Once the incident wave reaches the input bar-specimen interface, a complex wave reflection from both the input bar-specimen contact interface and from the input bar-specimen free surface takes wave, and the strain gage records the signal, which is termed the reflected wave ( $\varepsilon_r(t)$ ). A complex reverberation takes wave in the specimen between input bar-specimen interfaces and the specimen-output bar interface, until a strain of tensile waves are propagated to the output bar. The strain gage mounted on the output bar records the superposition of all the transmissions from the specimen-output bar interface and is termed as the transmitted wave ( $\varepsilon_t(t)$ ) [2].

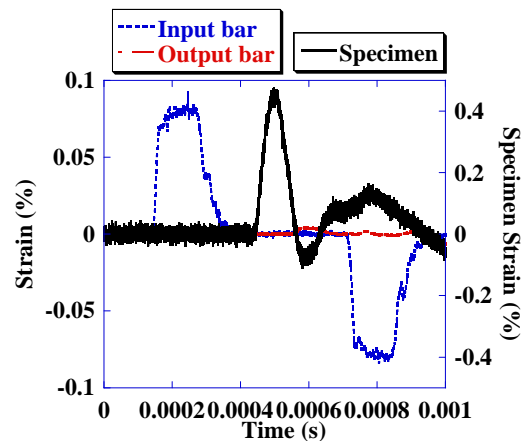


Fig.2 Strain gage signals obtained from a SHPB impact tensile test.

Fig.2 shows strain gage signals obtained from a SHPB impact tensile test. The one that incident wave, reflected wave and transmitted wave were chosen from Fig.2 shown in Fig.3.

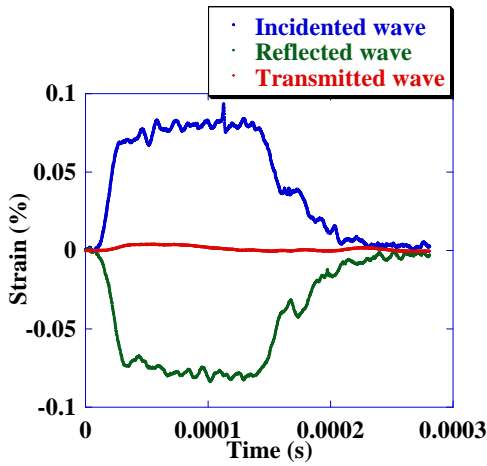


Fig.3 Strain-time curves (incident wave, reflected wave and transmitted wave)

Therefore, specimen stress, specimen strain and specimen strain rate can be shown by the following equations.

$$\sigma_s = \frac{E_o \varepsilon_t(t) A_o}{A_s} \quad (1)$$

$$\varepsilon_s = \frac{C_i \int_0^t \{\varepsilon_i(t') - \varepsilon_r(t')\} dt' - C_o \int_0^t \varepsilon_t(t') dt'}{l_s} \quad (2)$$

$$\dot{\varepsilon}_s = \frac{C_i \{\varepsilon_i(t) - \varepsilon_r(t)\} - C_o \varepsilon_t(t)}{l_s} \quad (3)$$

Here,  $C$  is a wave velocity.

Fig.4 shows stress-strain curves for unidirectional laminates under monotonic tensile test ( $\theta=0^\circ, 15^\circ, 30^\circ, 45^\circ, 60^\circ, 75^\circ$  and  $90^\circ$ ). It was found that the stress-strain curves of  $0^\circ$  specimen showed almost linear and little strain rate dependence. The off-axis and  $90^\circ$  specimens showed strain rate dependence.

Fig.5 shows stress-total strain and stress-elastic strain curves obtained from the monotonic tensile test on cross-ply laminates. On-axis specimens showed almost linear and little strain rate dependence stress-strain behavior. However, nonlinear and strain rate dependence appeared remarkably in the off-axis specimens. Fig.6 shows stress-total strain and stress-elastic strain curves obtained from the loading-unloading test on cross-ply laminates. In the cross-ply laminates, large nonlinearity was observed in off-axis specimens.

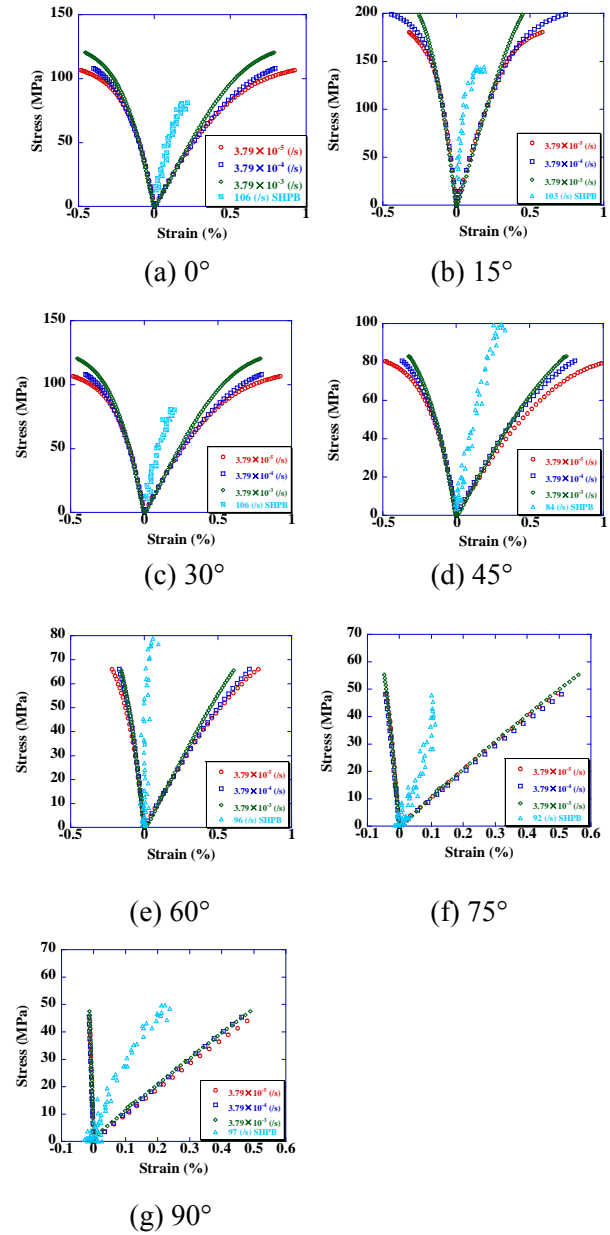


Fig.4 Stress-strain curves for unidirectional laminates at various strain rates (a)  $0^\circ$ , (b)  $15^\circ$ , (c)  $30^\circ$ , (d)  $45^\circ$ , (e)  $60^\circ$ , (f)  $75^\circ$  and (g)  $90^\circ$

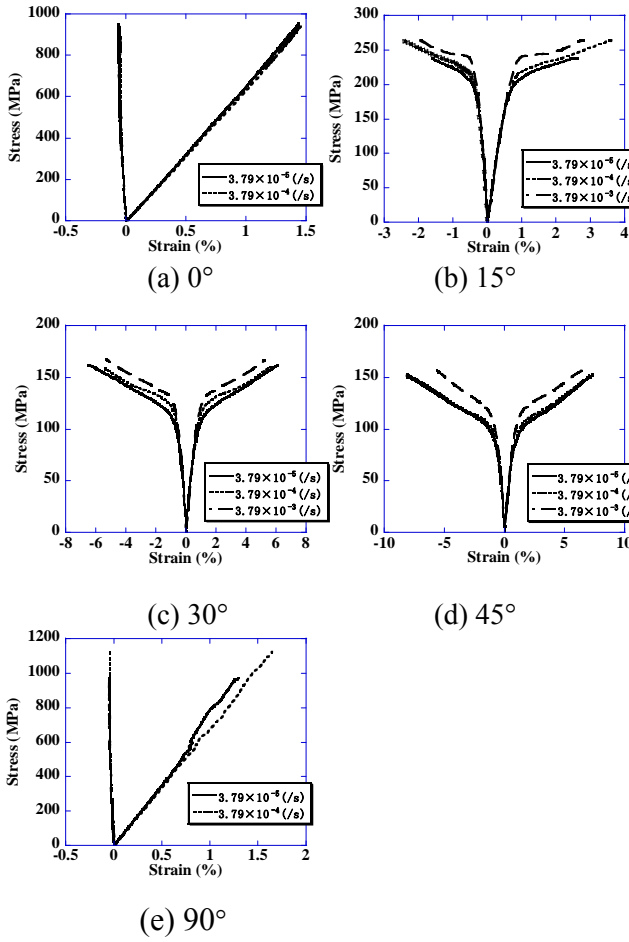


Fig.5 Stress-strain curves for cross-ply laminates obtained by monotonic tensile test (a) 0°, (b) 15°, (c) 30°, (d) 45° and (e) 90°

### 3.2 Modeling of stress-strain curves relation

In the present study, an attempt was made to model the nonlinear stress-strain relation under off-axis tensile loading on unidirectional laminates to characterize strain rate dependence by using the one-parameter plasticity model [3]. Here, one-parameter plasticity model is outlined.

A yield function that is quadratic in stresses is assumed for the 3-D fiber composites as

$$\begin{aligned}
 2f = & a_{11}\sigma_{11}^2 + a_{22}\sigma_{22}^2 + a_{33}\sigma_{33}^2 \\
 & + 2a_{12}\sigma_{11}\sigma_{22} + 2a_{23}\sigma_{22}\sigma_{33} + 2a_{13}\sigma_{11}\sigma_{33} \\
 & + 2a_{44}\sigma_{23}^2 + 2a_{55}\sigma_{13}^2 + 2a_{66}\sigma_{12}^2 = k
 \end{aligned} \quad (4)$$

where  $k$  is a state variable and  $\sigma_{ij}$  refer to the stress in the material principle directions. By using the associated flow rule, the incremental plastic

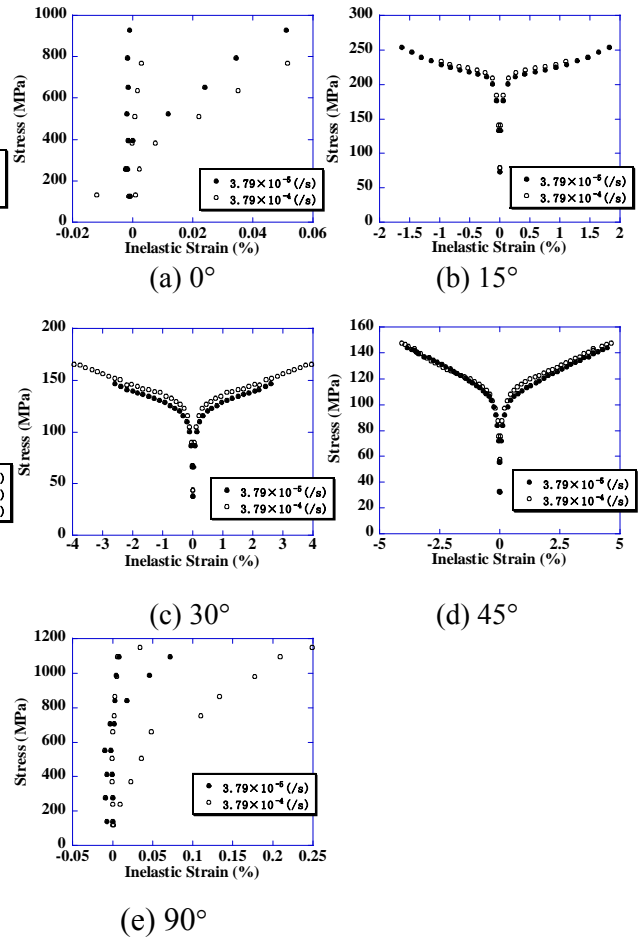


Fig.6 Stress-strain curves for cross-ply laminates obtained by loading-unloading test (a) 0°, (b) 15°, (c) 30°, (d) 45° and (e) 90°

strains can be written in terms of the plastic potential  $f$  as

$$d\varepsilon_{ij}^p = \frac{\partial f}{\partial \sigma_{ij}} d\lambda \quad (5)$$

where the superscript  $p$  denotes plasticity, and  $d\lambda$  is a proportionality factor. The increment of plastic work per unit volume is given by

$$dW^p = \sigma_{ij} d\varepsilon_{ij}^p = 2f d\lambda \quad (6)$$

Let the effective stress  $\bar{\sigma}$  be defined as

$$\bar{\sigma} = \sqrt{3f} \quad (7)$$

The effective plastic strain increment  $d\varepsilon^p$  can be defined such that

$$dW^p = \sigma_{ij} d\varepsilon_{ij}^p = \bar{\sigma} d\varepsilon^p \quad (8)$$

Substitution of equations (6) and (7) into (8) yields

$$d\bar{\varepsilon}^p = \frac{2}{3}\bar{\sigma}d\lambda \quad (9)$$

and

$$d\lambda = \frac{3}{2}\left(\frac{d\bar{\varepsilon}^p}{d\bar{\sigma}}\right)\left(\frac{d\bar{\sigma}}{\bar{\varepsilon}}\right) \quad (10)$$

Consider a state of plane stress parallel to the  $x_1$ - $x_2$  plane, the plastic potential function reduces to

$$2f = a_{11}\sigma_{11}^2 + a_{22}\sigma_{22}^2 + 2a_{12}\sigma_{11}\sigma_{22} + 2a_{66}\sigma_{12}^2 \quad (11)$$

The plastic strain increments are obtained from equations (5) and (11) as

$$\begin{Bmatrix} d\varepsilon_{11}^p \\ d\varepsilon_{22}^p \\ d\gamma_{12}^p \end{Bmatrix} = \begin{bmatrix} a_{11} & a_{12} & 0 \\ a_{12} & a_{22} & 0 \\ 0 & 0 & 2a_{66} \end{bmatrix} \begin{Bmatrix} \sigma_{11} \\ \sigma_{22} \\ \sigma_{12} \end{Bmatrix} d\lambda \quad (12)$$

Experimental data show that fiber composite behaves linearly up to failure in the fiber direction. It is thus reasonable to assume that

$$d\varepsilon_{11}^p = 0 \quad (13)$$

which leads to the condition

$$a_{11} = a_{12} = 0 \quad (14)$$

The condition of equation (13) is used to reduce the plastic potential function equation (11) to

$$2f = \sigma_{22}^2 + 2a_{66}\sigma_{12}^2 \quad (15)$$

in which, without loss of generality, we further set  $a_{22}=1$ . Therefore,  $a_{66}$  of the plasticity parameter remains in the plasticity potential. This is called one-parameter plasticity model.

Let  $x$ -axis be the uniaxial loading direction which makes an angle  $\theta$  with the fiber direction  $x_1$ -axis. The stress referring to the material principal axes are

$$\begin{cases} \sigma_{11} = \cos^2 \theta \sigma_x \\ \sigma_{22} = \sin^2 \theta \sigma_x \\ \sigma_{12} = -\sin \theta \cos \theta \sigma_x \end{cases} \quad (16)$$

where  $\sigma_x$  is the applied stress.

Substitutions of equation (16) into equations (7) and (15) yield

$$\bar{\sigma} = h(\theta)\sigma_x \quad (17)$$

and

$$d\bar{\varepsilon}^p = \frac{2}{3}h(\theta)\sigma_x d\lambda \quad (18)$$

respectively. In equations (17) and (18)

$$h(\theta) = \left[ \frac{3}{2}(\sin^4 \theta + 2a_{66} \sin^2 \theta \cos^2 \theta) \right]^{1/2} \quad (19)$$

From the coordinate transformation law, we have

$$d\varepsilon_x^p = d\varepsilon_{11}^p \cos^2 \theta + d\varepsilon_{22}^p \sin^2 \theta - d\gamma_{12}^p \sin \theta \cos \theta \quad (20)$$

Comparing equations (9), (16), (17) and (19) we find that

$$d\bar{\varepsilon}^p = \frac{d\varepsilon_x^p}{h(\theta)} \quad (21)$$

it now shown that the effective stress-effective plastic strain relation can be obtained by using the stress and the plastic strain obtained by the monotonic tension test. Since the effective stress-effective plastic strain curve should be unique in monotonic loading for a given material, the parameter  $a_{66}$  must be chosen so that the resulting effective stress-effective plastic strain relations are independent of  $\theta$ . Fig.7 shows the obtained effective stress-effective plastic strain relation. In the figure, fitting curves are also shown. The effective stress-effective plastic strain relations are fitted in the form

$$\bar{\varepsilon}^p = A(\bar{\sigma})^n \quad (22)$$

where  $A$  and  $n$  are constants. The parameter used is listed in Table 1. The influence of the loading rate appears as a difference in effective stress-effective plastic strain relation. It is confirmed that stress-inelastic strain relation of the unidirectional laminates can be modeled by the one-parameter plasticity model.

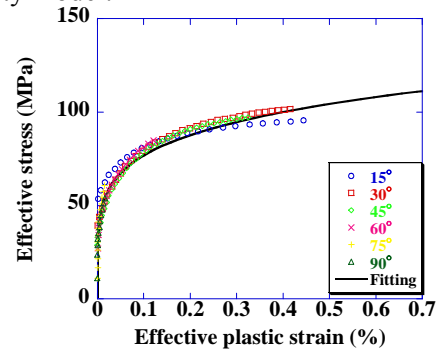


Fig.7 Effective stress-effective plastic strain curves for unidirectional laminates ( $3.79 \times 10^{-5}$ (/s))

Table 1 parameters used in the one-parameter plasticity model

Strain rate (/s)	$a_{66}$	$A$ (MPa $^{-n}$ )	$n$
$3.79 \times 10^{-5}$	1.45	$1.14 \times 10^{-11}$	5.27
$3.79 \times 10^{-4}$	1.45	$9.05 \times 10^{-12}$	5.27
$3.79 \times 10^{-3}$	1.45	$2.35 \times 10^{-12}$	5.27

However, the amplitude  $A$  is a function of strain rate. Therefore, a viscoplasticity model [4] relation the effective stress and effective plastic strain is written as

$$\bar{\varepsilon}^p = 10^a (\log(\dot{\bar{\varepsilon}}^p))^2 + b (\log(\dot{\bar{\varepsilon}}^p)) + c \left( \frac{\bar{\sigma}}{A} \right)^n \quad (23)$$

Fig.8 shows amplitude  $A$  as a function of effective plastic strain rate on the log-log scale. Each parameter is decided from the fitting curve. The parameter used is listed in Table 2.

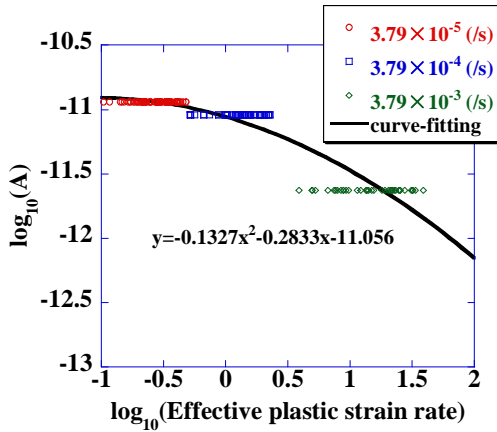


Fig.8 Log-log plot for determining the parameters in the viscoplasticity model

Table 2 parameters used in the viscoplasticity model

a	b	c
-0.133	-0.283	-11.1

Fig.9 showed stress-strain curves for unidirectional laminates. The prediction of the stress-strain curve of SHPB test from three strain rates ( $\square = 3.79 \times 10^{-5}$ (/s),  $3.79 \times 10^{-4}$ (/s) and  $3.79 \times 10^{-3}$ (/s)) is also shown in the figure. By using this model, the stress-strain relation of a different loading rate can be predicted.

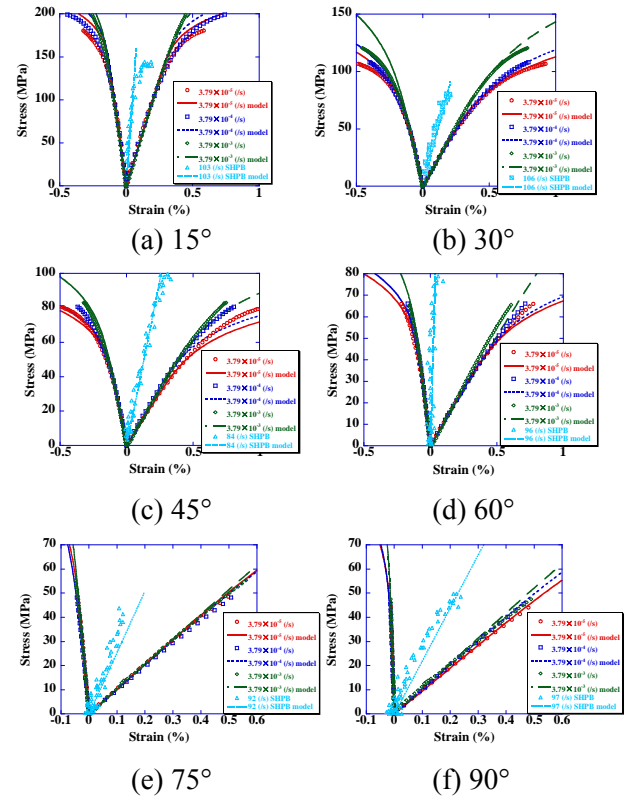


Fig.9 Stress-strain curves for unidirectional laminates

Here, an attempt is made to predict stress-strain relation for the cross-ply laminate by combining viscoplastic models for the unidirectional laminate with the laminate theory.

Considering the total strain is composed of the linear elastic strain and the inelastic strain, the compliance matrix of unidirectional laminates can be written by the following equations.

$$\{\dot{\varepsilon}\} = [S^{ep}] \{\dot{\sigma}\} \quad (24)$$

$$[S^{ep}] = \begin{bmatrix} S_{11} & S_{12} & 0 \\ S_{22} + \frac{9\sigma_{22}^2}{4H_p\bar{\sigma}^2} & \frac{9a_{66}\sigma_{22}\sigma_{12}}{2H_p\bar{\sigma}^2} \\ sym. & S_{66} + \frac{9a_{66}^2\sigma_{12}^2}{H_p\bar{\sigma}^2} \end{bmatrix} \quad (25)$$

The inverse of equation (24) is

$$\{\dot{\sigma}\}^k = [Q^{ep}]^k \{\dot{\varepsilon}\}^k \quad (26)$$

Here, it is described in the laminate coordinate system as follows by using the coordinate transformation method,

$$\{\dot{\tilde{\sigma}}\}^k = [T_{\sigma}^k]^{-1} [Q^{ep}]^k [T_{\varepsilon}^k] \{\dot{\tilde{\varepsilon}}\}^k = [\tilde{Q}^{ep}]^k \{\dot{\tilde{\varepsilon}}\}^k \quad (27)$$

and

$$[T^{\sigma}] = \begin{bmatrix} m^2 & n^2 & 2mn \\ n^2 & m^2 & -2mn \\ -mn & mn & m^2 - n^2 \end{bmatrix} \quad (28)$$

$$[T^{\varepsilon}] = \begin{bmatrix} m^2 & n^2 & mn \\ n^2 & m^2 & -mn \\ -2mn & 2mn & m^2 - n^2 \end{bmatrix} \quad (29)$$

$(m = \cos \theta, \quad n = \sin \theta)$

Here, the strain of the kth layer is the same as the strain of the laminate and the relation to the stress can be expressed as follows.

$$\{\dot{\tilde{\varepsilon}}\} = \{\dot{\tilde{\varepsilon}}\}^k \quad (30)$$

$$\{\dot{\tilde{\sigma}}\} = \frac{\sum_{k=1}^N t_k \{\dot{\tilde{\sigma}}\}^k}{\sum_{k=1}^N t_k} \quad (31)$$

Therefore, stress-strain relation of the laminate can be described by the following equation.

$$\{\dot{\tilde{\sigma}}\} = \frac{\sum_{k=1}^N t_k [\tilde{Q}^{ep}]^k}{\sum_{k=1}^N t_k} \{\dot{\tilde{\varepsilon}}\} \quad (32)$$

Stress-strain relation of the cross-ply laminate predicted. Fig.10 shows the stress-strain curves. It can be confirmed that the stress to a certain strain is also high when the strain rate is high. The difference between experimental results and prediction of the model grows in the plastic region. It is thought that it is not consider the influence of damage as one of these factors. It is thought that the predictability improves by considering the influence of damage on stress-strain relation.

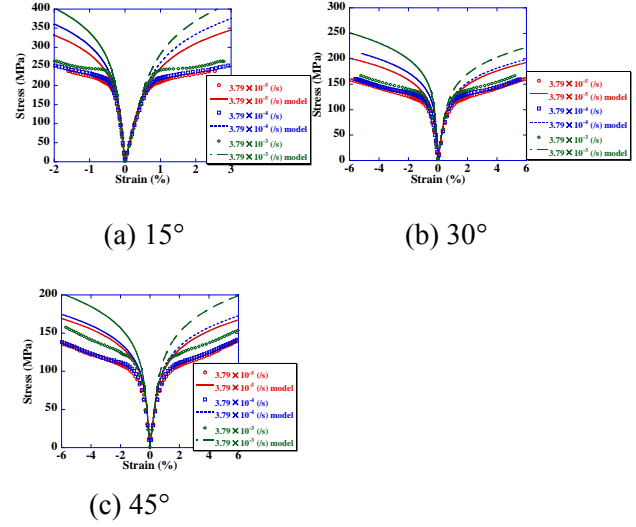


Fig.10 Stress-strain curves for cross-ply laminates

#### 4 Conclusions

In the present study, effect of loading rate on the mechanical response of CFRP laminates is evaluated experimentally.

(1) A viscoplasticity model is used to characterize the behavior of the unidirectional laminate.

(2) By combining the viscoplasticity model and the lamination theory, stress-strain relation of cross-ply laminate is predicted and compared with the experimental results.

#### References

- [1] Haomouda A.M.S. and Hashmi M.S.J., "Testing of composite materials at high rate of strain: advances and challenges" *Journal Material Processing Technology*, Vol.77, pp 327-336, 1998.
- [2] Gama B.A., Lopatnikov S.L. and Gillespie Jr. J.W., "Hopkinson bar experimental technique: A critical review" *Applied mechanical review*, vol.57, pp 223-250, 2004.
- [3] Sun C.T. and Chen J.L., "A Simple Flow Rule for Characterizing Nonlinear Behavior of Fiber Composites" *Journal of Composite Materials*, Vol.23, pp 1009-1020, 1989.
- [4] Tsai J. and Sun C.T., "Constitutive model for high strain rate response of polymeric composites" *Composites Science and Technology*, Vol.62, pp 1289-1297, 2002.